Removal of rhodamine B from aqueous solutions using vanadium pentoxide/titanium butyl oxide hybrid xerogels

Surayya Mukhtar[†], Mona Liu, Jie Han, and Wei Gao[‡]

[1] *Department of Physics, Allama Iqbal Open University, H-8 sector, Islamabad, Pakistan*
[2] *Department of Chemical and Materials Engineering, the University of Auckland, Auckland* 1142, *New Zealand*

(Received 28 November 2016; revised manuscript received 31 January 2017; published online 12 April 2017)

A stable and insoluble $V_2O_5{\cdot}nH_2O$/tetra-n-butyl titanate (TBO) hybrid xerogel was synthesized by the sol–gel method. This novel material proved to be an efficient absorbent with an absorption capacity of 179 $mg{\cdot}g^{-1}$ for Rhodamine B (RhB) in water due to its unique layered structure, which can effectively accommodate RhB molecules between its layers as demonstrated by XRD and FTIR spectroscopic analyses.

Keywords: layered material, V_2O_5 xerogel, rhodamine B, absorption

PACS: 82.70.Gg **DOI:** 10.1088/1674-1056/26/5/058202

1. Introduction

Layered materials like clays, bentonite, saponite, montmorillonite, and layered double hydroxides (LDH) exhibit excellent intercalation properties due to their ion-exchange abilities and their flexible interlayer spacing that can accommodate guest molecules between the layers without affecting other structural features.[1–6] Vanadium pentoxide (V_2O_5) xerogels have a layered texture similar to that of clays. Their composition can be denoted as $V_2O_5 \cdot nH_2O$, where n represents the number of water molecules that reside between adjacent vanadium oxide layers. The interlayer spacing d between the bilayer slabs is highly sensitive to the water content, and expand or contract based on the intercalation or extraction of water molecules.[7] In contrast to clay minerals, which have intrinsic metal cations for exchange, $V_2O_5 \cdot nH_2O$ xerogels have only dissociable H_2O molecules, and are therefore acidic in nature.[8] and show a large cation exchange capacity of ~ 0.33 for monovalent cations.[9] V_2O_5 xerogels also offer a prodigious capacity for intercalating atoms as well as molecules of organic[10–13] and inorganic[9–14] substances. This property makes $V_2O_5 \cdot nH_2O$ xerogels different from three dimensional crystalline V_2O_5, which can only accommodate metal ions. Their easy synthesis, the abundance of the source materials and high intercalation capacity are the key factors that have marked V_2O_5 xerogels as suitable host materials for intercalation chemistry.[15]

The intercalation of organic dyes into the lamellar structure of a V_2O_5 xerogel for photoactive and lasing purposes has been reported by several authors.[16–18] But few reports are found in the literature on employing $V_2O_5 \cdot nH_2O$ xerogels as an absorbent material for the removal of organic dyes from waste water.[19,20] $V_2O_5 \cdot nH_2O$ xerogels exfoliate in water in a manner similar to clays, and form brown coloured colloidal suspensions that limit their use in decolourizing/cleaning of aqueous media. To effectively utilize the intercalation properties of this novel material to remove dyes from waste water, there is a need to develop a hybrid V_2O_5 xerogel that maintains its intercalation capacity while remaining insoluble in aqueous solutions.

It has been reported that an insoluble xerogel, characterized as $V_2O_{4.8} \cdot xH_2O$, can be synthesized by the reduction of fresh decavanadic acid with a reducing agent such as alcohol, acetone, hydrazine, etc.[21] Insoluble xerogels can also be prepared by the irreversible intercalation of tetrathiafulvaline (TTF) into $V_2O_5{\cdot}1.6H_2O$ in an ethanol/water mixture that acts as a solvent.[22] It was hypothesized that the TTF stabilizes the host V_2O_5 xerogel, and might form reduced vanadium oxide xerogels ($V_2O_{4.8-4.9} \cdot nH_2O$) that contain an abundant amount of water in a quite stable form. Furthermore, layered and stable vanadium metal oxide xerogels intercalated with tetravalent ions, with compositions $V_{1.67}M_{0.33}O_{5\pm\delta} \cdot nH_2O$ (M = Ti or Mo), have been prepared by the sol - gel method.[23] In another study, vanadium titanium oxide xerogels were formed by the sol–gel method using V_2O_5 and TiH_2 as starting materials. The composition and structure of the above solid solutions depend upon their contents: $V_{2-y}Ti_yO_{5-\delta} \cdot nH_2O$ ($0 < y < 1.33$, layered structure) and $Ti_{1-y}V_yO_{2+y} \cdot nH_2O$ ($0 < y < 0.25$, anatase structure).[24] While $V_{2-y}Ti_yO_{5-\delta} \cdot nH_2O$ forms stable gels, the stacking order of the layers was found to be affected by an increase in the Ti content.

In this study, an insoluble hybrid V_2O_5 xerogel is prepared by the reduction of a $V_2O_5 \cdot nH_2O$ xerogel using a solution of tetra-n-butyl titanate (TBO) mixed with ethanol. This

[†]Corresponding author. E-mail: surayya.mukhtar@aiou.edu.pk
[‡]Corresponding author. E-mail: w.gao@auckland.ac.nz

© 2017 Chinese Physical Society and IOP Publishing Ltd

novel material is proposed as an efficient absorbent for the toxic cationic dye rhodamine B (RhB) in aqueous solutions.

2. Experimental

The vanadium oxide xerogel ($V_2O_5 \cdot nH_2O$) was synthesized by the sol–gel method, as described in previous literature.[25–27] In a typical synthesis, commercially purchased orthorhombic V_2O_5 powder (99.6%, Sigma Aldrich) was added into distilled water and mixed well to prepare a 0.05 M solution. Then, 15 mL of H_2O_2 (30 wt %) was added drop-wise to the solution and stirred for 1 h, leading to the formation of a reddish-brown sol. This was heated at 80 °C for 9 h to evaporate the water slowly. The final product was a reddish brown solid, which was ground into a fine powder for further use. In addition, 0.2 g of TBO (97%, Sigma Aldrich) was slowly dropped into 10 mL of anhydrous ethanol (99.7%) to form a transparent solution. Next, the V_2O_5 xerogel powder (0.2 g) prepared above was dispersed in the TBO/ethanol solution by ultrasonication for 30 min. The solution was kept overnight to dry under ambient conditions. A light green coloured hybrid xerogel was obtained after the drying step, which was again ground to a fine powder with the help of a spatula.

Absorption spectroscopy was performed by considering the RhB dye as the absorbate and the hybrid xerogel prepared above as the absorbent. A RhB stock solution (120 mg·L^{-1}) was initially prepared. It was diluted further to 12 mg·L^{-1} by adding deionized (DI) water. The hybrid xerogel (10 mg) was added into 30 mL of this diluted RhB solution. Experiments were performed in a dark chamber to eliminate the effect of light. The mixed solution was stirred via a magnetic stirrer at 100 rpm to facilitate mass transfer. At intermittent time intervals, $\sim$ 4 mL of the sample solution was extracted and centrifuged at 14000 rpm for 7 min to separate the absorbent from the solution. The absorption spectrum of the supernatant solution was then analysed by using an Agilent UV–Vis spectrophotometer 8745. A calibration curve of the absorbance versus RhB concentration was established by preparing standard RhB aqueous solutions and measuring their absorption peak at 553 nm (see Fig. A1 in Appendix A).

Nitrogen physic-sorption measurements were conducted on a Micromeritics Tristar 3000 instrument. Surface areas and pore sizes were calculated from the isotherms by following the Brunauer–Emmett–Teller (BET) and Barrett–Joyner–Halenda (BJH) methods, respectively. The zeta potential of the hybrid xerogel was measured on a Malvern Zetasizer Nano ZS.

Structural analysis of the xerogel was carried out using a D2 Phaser Bruker x-ray diffractometer (XRD). The 2θ angle range was set between 5° and 45°. XRD patterns at low angles, i.e. starting from 2°, were obtained by using a D8 Advance Bruker XRD. Both XRDs were used in locked couple $2\theta/\theta$ mode with Cu $K\alpha$ radiation. A Perkin Elmer Spectrum 100 FTIR spectrometer was used in the attenuated total reflectance (ATR) mode to investigate the chemical structure of the hybrid xerogel. The FTIR spectra were obtained in the wave number range of 400–4000 cm^{-1}, with a resolution of 4 cm^{-1}.

3. Results and discussion

3.1. UV–Vis absorption spectroscopy

Figure 1 shows the absorption spectra of the diluted RhB ($C_o = 12$ mg·L^{-1}) aqueous solutions stirred with pure and hybrid V_2O_5 xerogels and measured at different time intervals. An aqueous solution of the pure xerogel shows a broad absorption spectrum in the visible region (Fig. 1(a)) that is due to the brown coloured ions and light scattering in the colloidal suspension.[28] Moreover, two absorption bands in the ultraviolet region at 285 nm and 385 nm represent the electron charge transition from O $\rightarrow$ V^{5+} in the xerogel in the presence of excess water.[10] The RhB aqueous solution that was not stirred with the xerogel shows a maximum absorption peak at 553 nm. It can be observed that the maximum absorption band of RhB shifted from 553 nm to 573 nm when stirred with the pure V_2O_5 xerogel solution. However, the rest of the absorption spectrum is similar to the absorption curve of the pure xerogel aqueous solution. In contrast, the intensity of these bands is negligible for the RhB aqueous solution stirred with the hybrid V_2O_5 xerogel, for which the main absorption band of RhB located at 553 nm was not shifted. This characteristic of the hybrid xerogel is beneficial for employing it as a matrix for the intercalation of the dye molecules.[16] Moreover, the insoluble V_2O_5 hybrid xerogel did not form a brown coloured colloidal suspension, as shown in Fig. 2. After 30 min, $\sim$ 85% and 95% of the RhB were removed from the solutions stirred with the pure and hybrid V_2O_5 xerogels, as measured at $\lambda_{max} = 573$ nm and 553 nm, respectively. The RhB solution with the pure xerogel was stirred for another 100 min, but it did not show any further absorption of RhB. However, the intensity of the peaks in the UV region increased (Fig. 1(a)).

When the RhB aqueous solution was mixed with the pure and hybrid xerogels, the pH values of the solutions were noted as 3.4 and 4, respectively. The point of zero charge (PZC) for the V_2O_5 xerogel is reported as approximately pH 2.[8] At the PZC, a substance is considered to be neutral. At pH>PZC, a substance exhibits anionic behaviour. In the present study, the zeta potential of the pure and hybrid xerogels at their respective pH values was calculated to be in the range of -24 mV to -35 mV. This indicates that the xerogel particles have negatively charged surfaces in the pH range in question. In an aqueous solution, RhB can exist in three different ionic forms,

i.e. protonated RBH^+, neutral zwitterionic $RhB^{\pm}$ and colourless lactone. The presence of these forms depends on the pH, concentration and temperature of the environmental solution (prototropic forms of RhB are shown in Fig. A2, Appendix A). At pH < 4, the RhB ions are in the protonated and monomeric molecular form. Thus, they can enter into the pore structure easily. At a pH > 4, the zwitterionic form of RhB exists in water, and causes the aggregation of RhB to form a larger molecular unit (dimer) which is not easily adsorbed by the sorbate.[29] It is therefore speculated that at the pH values measured in the hybrid xerogel solution, RhB^+ cations were attracted towards the negatively charged V_2O_5 layers via electrostatic forces, leading to dominating ion exchange interactions with the physically bonded water molecules and H_3O^+ ions present in the xerogel.

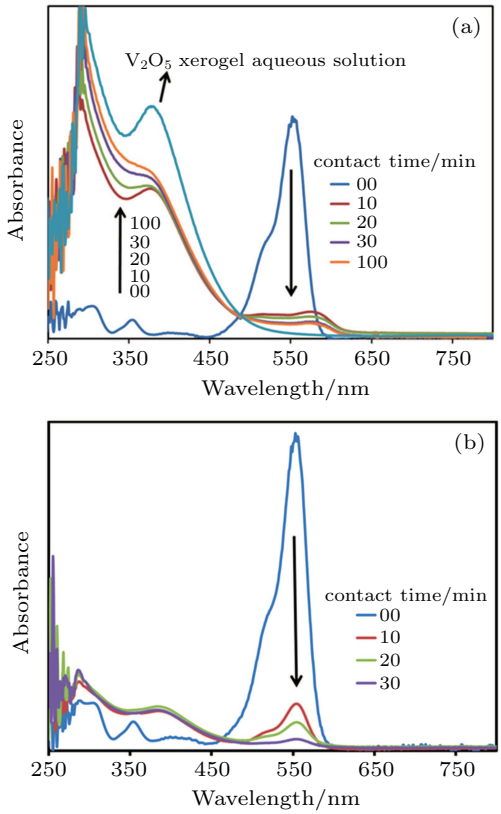


Fig. 1. (color online) UV–Vis absorption spectra of RhB aqueous solutions with an initial concentration $C_o = 12$ mg·L^{-1}, stirred with pure (a) and V_2O_5 hybrid (b) xerogels, as a function of contact time.

The average pore diameter (d_{por}), specific surface area (S_{BET}) and average pore volume (V_{por}) of the pure xerogel were calculated by using the BET and BJH methods, and were found to be 33.8 nm, 1.25 m^2·g^{-1} and 4.17×10^{-5} m^3·g^{-1}, respectively. The addition of TBO into the V_2O_5 xerogel induced a dramatic increase in the S_{BET} and V_{por} values to 27.57 m^2·g^{-1} and 3.72×10^{-4} m^3·g^{-1}, respectively. Whereas the pore diameter for the hybrid xerogel was decreased to 7.25 nm, but the number of pores was increased as observed by increase in pore volume. The S_{BET} for the hybrid xerogel was more than 22 times larger than that of the pure xerogel. The significant increase of the surface area and pore volume of the hybrid xerogel compared to the pure xerogel indicates that the former possess a more hollow structure and provides more reaction sites for the target dye molecules. The pore diameter of xerogel is sufficient for the adsorption of monomers of RhB at the tested pH of aqueous solution. Moreover, The UV–Vis spectroscopy results confirm that the hybrid xerogel has more absorption capacity for the RhB dye than the pure xerogel. While the pore diameter of the hybrid xerogel was smaller at 7.25 nm, the number of pores was larger, as indicated by the increase in the total pore volume. Furthermore, the pore diameter of the xerogel is sufficient for the adsorption of RhB monomers at the measured pH of the aqueous solution. It is speculated that the absorption of RhB by the hybrid xerogel takes place in two steps: initially the RhB is adsorbed through surface diffusion over the V_2O_5 hybrid xerogel, and secondly, the dye monomers intercalate between the layers of the xerogel.

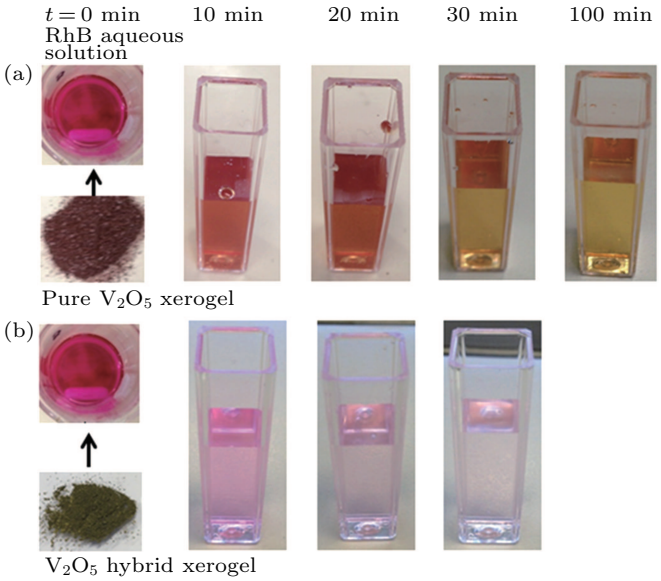


Fig. 2. (color online) Images of RhB aqueous solutions stirred with the pure V_2O_5 xerogel (a), and hybrid V_2O_5 xerogel (b) at successive time intervals.

3.2. Effect of initial dye concentration and absorbent dosage on the absorption of RhB by the hybrid V_2O_5 xerogel

To investigate the effect of different initial concentrations and absorbent dosages on the RhB absorption capacity of the hybrid V_2O_5 xerogel at a fixed pH = 4, a series of experiments were performed at room temperature. RhB aqueous solutions with a volume of 50 mL and initial concentrations 36, 48, 60, 72, 84, and 120 mg·L^{-1} were prepared. A fixed amount of the hybrid xerogel (30 mg) was added to each solution, which was then agitated in a shaker at a speed of 200 rpm for 24 h. Once the equilibrium state was reached, the amount of RhB

absorbed by a unit mass of the absorbent q_e (mg·g^{-1}) was calculated by the following relation:

$$q_e = \frac{V(C_o - C_e)}{M},$$

where V is the volume of the solution, M is the mass of absorbent, C_o is the initial concentration, and C_e is the concentration of the RhB at equilibrium time t.

The uptake of RhB increases linearly from 58 mg·g^{-1} to 134 mg·g^{-1} for initial dye concentrations in the 36 mg·L^{-1} to 84 mg·L^{-1} range, but starts to deviate from the linear trend when the dye concentration is increased further to 120 mg·L^{-1}, as shown in Fig. 3(a). Therefore, the above value indicates the saturation state of the absorbent corresponding to the maximum absorption of the dye.

It must also be noted that the dose of absorbent in a RhB solution also affects its absorption capacity. For a fixed initial dye concentration of 120 mg·L^{-1}, the absorbent amount was varied from 10 mg to 60 mg. In this case, the uptake of RhB was observed to be in the range from 179 mg·g^{-1} to 99 mg·g^{-1}, respectively (Fig. 3(b)). These results indicate a high RhB absorption capacity for the hybrid xerogel. From the graph in Fig. 3(b), it can be seen that the absorption capacity of the hybrid xerogel q_e has a somewhat inversely proportional relationship with the sorbate dose in the range 30 mg–60 mg, i.e., q_e decreases with increasing sorbate dose. This indicates that the sorbate has a much larger absorption surface available for the accommodation of the RhB dye molecules. For sorbate doses below 30 mg, the increase in the absorption capacity q_e of the xerogel is barely noticeable (e.g. 171 mg·g^{-1} to 179 mg·g^{-1} for sorbate doses from 20 mg to 10 mg, respectively). This result explains the non-linear trend observed in Fig. 3(a) at the saturation state for RhB dye absorption of the hybrid xerogel.

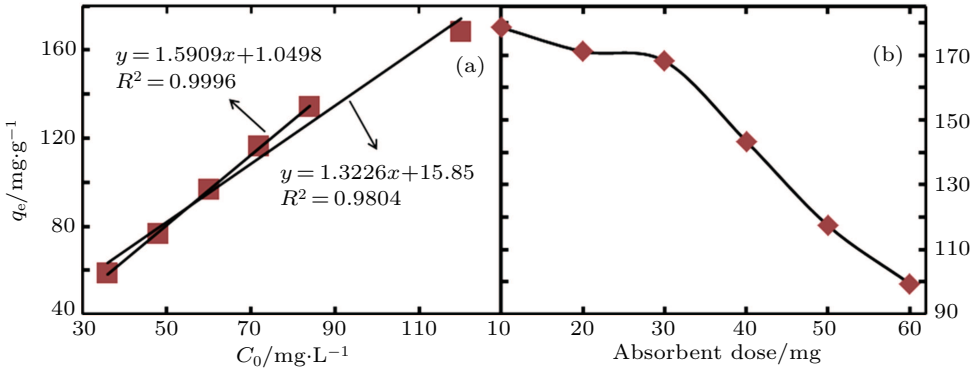


Fig. 3. (color online) The effect of initial dye concentration (a) and absorbent dose (b) on RhB uptake by the hybrid V_2O_5/TBO xerogel.

3.3. Desorption

At the equilibrium time of 24 h, the hybrid V_2O_5 xerogel had absorbed 117 mg·g^{-1} of RhB from the concentrated RhB solution (120 mg·L^{-1}). The RhB-loaded xerogel in the solution was allowed to settle for 2 h after absorption. The supernatant was carefully extracted using a set of transfer pipettes, and the precipitates were dried in an oven at 50 °C for 2 h. Two solvents, DI water and ethanol, were used in the desorption study. The solutions were gently stirred using a magnetic stirrer at 100 rpm for 24 h in a dark chamber. As shown in Fig. 4, it was observed that approximately 4 mg·g^{-1} and 65 mg·g^{-1} of absorbed RhB were desorbed from the dye loaded hybrid xerogel in DI water and ethanol, respectively. These values are equivalent to 3.41% and 55.5% of the total amount of the absorbed dye (117 mg·g^{-1}). The results indicate that after desorption of the dye, the xerogel can be reused for absorption. Furthermore, desorption studies provide insights into the absorption mechanism, i.e., whether it is physisorption or chemisorption. If desorption readily occurs in neutral water, then the absorbate is likely to be held on the absorbent by weak bonds. On the other hand, if the absorbate desorbs only in chemical reagents, it is an indication of stronger bonding between the absorbate and absorbent.[30] Hence, the above

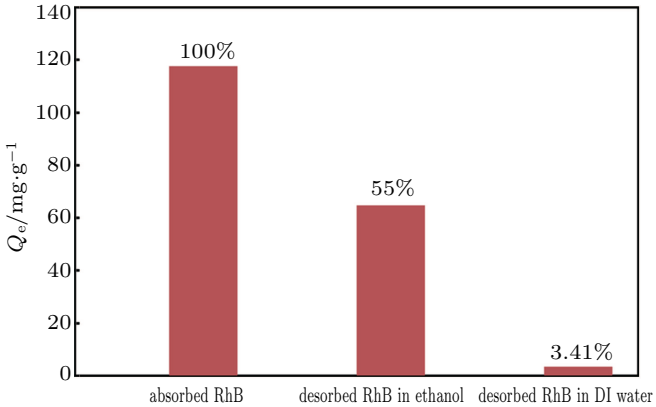


Fig. 4. (color online) Desorption of RhB from the V_2O_5/TBO hybrid xerogel in DI water and ethanol solvents.

results indicate that the absorption of RhB was driven by a strong binding force between RhB and the hybrid xerogel. Moreover, while the recovery of an organic cation may not be easily done using inorganic cations, one organic cation may be able to replace another.[31]

3.4. XRD results

The XRD patterns reflect the well-defined lamellar structure of the pure V_2O_5 xerogel in the *c* direction, as indicated by the strong (001) peak at $2\theta = 7.47°$ and similar reflections of (003), (004) and (005) at higher angles (Fig. 5(a)). The peaks delineate the orthorhombic $V_2O_5 1.6H_2O$ hydrate according to the data in the JCP2-2CA database (pdf file No: 040-1296).

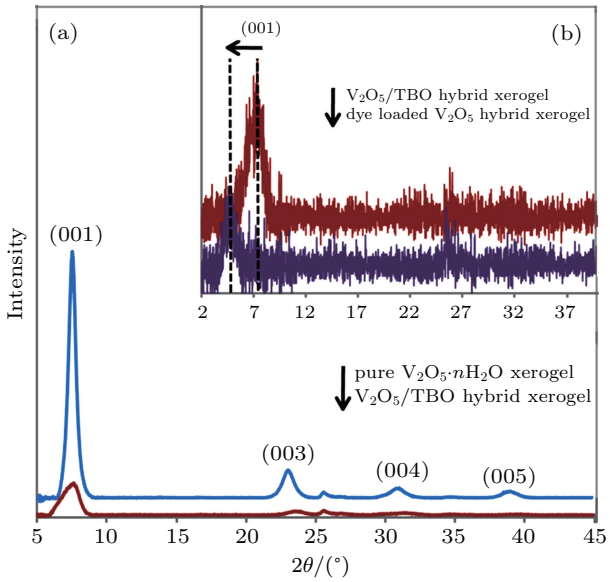


Fig. 5. (color online) (a) XRD patterns of the pure V_2O_5 xerogel, V_2O_5/TBO hybrid xerogel and dye loaded hybrid xerogel. (b) Increase in the *d* spacing as measured by the shift in the (001) peak in the RhB loaded V_2O_5/TBO xerogel.

The substitution of titanium for vanadium in the V_2O_5/TBO hybrid xerogel destroys the stacking order of the lattice in the *c* direction, as shown by a decrease in the intensity of the 00l peaks.[24] Moreover, compared to the pure xerogel, the interlayer spacing *d* decreased from 11.76 Å to 11.58 Å in the hybrid V_2O_5/TBO xerogel. This indicates that during dispersion of the V_2O_5 xerogel in the TBO/ethanol solution, loosely bonded water molecules were ejected from the interlayer regions of the xerogel, while Ti^{4+} ions were intercalated between the layers to form V–O–Ti layers.[23] It is known that guest species do not always change the interlayer spacing or improve the stacking order. Instead, such changes depend on the chemical nature of the guest and host species, as well as the reactions taking place between them.[32] A redox intercalation, which reduces V^{5+} to V^{4+} or forms VO^{2+} ions in the xerogel, can be suggested in this case. The change in the xerogel colour from brown to green is an indication of the reduction process, as shown in Fig. 2. It is speculated that Ti^{4+} ions are connected to oxygen atoms in the xerogel by strong covalent or ionic bonds, in contrast to the weak physical bonds of the water molecules. The strong bonding between the vanadium oxide layers due to the presence of Ti^{4+} ions stabilizes the V_2O_5 xerogel, leading to the production of an insoluble hybrid xerogel.

The XRD pattern in Fig. 5(b) shows a shift of the (001) peak of the V_2O_5/TBO hybrid xerogel from $2\theta = 7.28°$ to 4.59° (d = 11.58 Å to 19.24 Å) after the absorption of the RhB^+ cations. Taking into account the dimensions of the RhB^+ ion (length: 18 Å, base: 7 Å),[30] and the increase in the interlayer spacing *d*, we can reasonably speculate that either the intercalation of monomeric and dimeric forms of RhB^+ or coexistence of both is the reason for the above observation.[33,34] These results are further confirmed by FTIR spectroscopy, as discussed in the next section. The pure xerogel absorbs water molecules along with the RhB molecules from the aqueous solution due to its flexible layered structure, and forms a colloidal solution upon swelling. In contrast, the hybrid xerogel only accommodates the RhB molecules via exchange of hydronium ions present between the layers. The stable structure of the hybrid xerogel does not allow further absorption of water molecules.

3.5. FTIR spectroscopy

The FTIR results of the pure vanadium oxide xerogel showed a broad stretching band υ_s at 3600–2500 cm^{-1} due to O–H ions (Fig. 6(a)). A narrow band at 1610 cm^{-1} describes the water molecules that are chemically bonded to the oxide network. Four bands can be observed in the wavenumber range 1000–400 cm^{-1}. The terminal oxygen symmetric stretching band υ_s of V=O, with the main peak at 980 cm^{-1} and a shoulder band at 923 cm^{-1}, indicates the presence of mixed valance V^{4+} and V^{5+} ions. The asymmetric and symmetric stretching bands of the bridging oxygen atoms V–O–V are also shifted to lower frequencies of 719 cm^{-1} and 427 cm^{-1} from their typical band positions at 764 cm^{-1} and 527 cm^{-1}, respectively.[35] The reduced V^{4+} ions might have

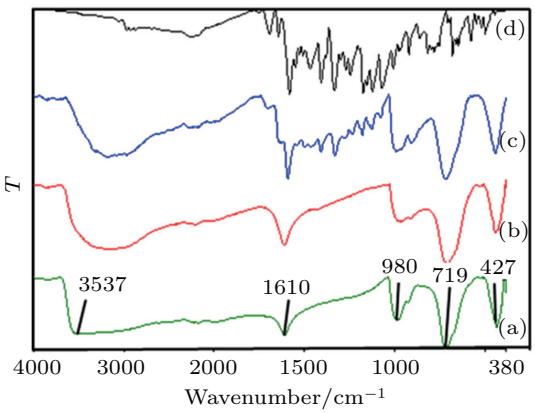


Fig. 6. (color online) FTIR spectra of the pure V_2O_5 xerogel (a), V_2O_5/TBO hybrid xerogel (b), RhB loaded V_2O_5/TBO hybrid xerogel (c) and RhB in its dry form (d).

been produced during the slow heat treatment of the sol during the synthesis of the V_2O_5 xerogel. The presence of O–H vibration modes in the FTIR spectrum of the hybrid xerogel indicate that a large number of water molecules are still present in the interlayer space of the xerogel, even after treatment with TBO (Fig. 6(b)). The broadness of the V=O band in the hybrid xerogel, compared to that of the pure V_2O_5 xerogel, indicates weaker V=O bonding. FTIR confirmed that the Ti^{4+} ions were inserted in the interlayers of the V_2O_5 xerogel,[24] and reduced the V^{5+} ions to V^{4+} by electron transfer in a manner similar to other metal cations such as Li, Na and Mg.[36] The size of the reduced vanadium ion, V^{4+}, is larger than the V^{5+} ion, and causes the expansion of the V=O bond. The polarity of the V–O–V bond is also affected by these structural changes, as observed by the shifting of the bands to lower wavenumbers, i.e. from 719 cm^{-1} to 707 cm^{-1} in the pure and hybrid xerogels, respectively. The IR spectrum of the dyeloaded hybrid xerogel clearly shows several bands belonging to RhB (Fig. 6(c)), which shows the intercalation of the RhB molecules within the layers of the xerogel. Moreover, a decrease in the intensity of bands corresponding to water molecules indicates replacement of the water molecules with the dye molecules. The bands belonging to the RhB molecules are also shifted slightly from their original positions (Fig. 6(d)). These band shifts are ascribed to the interaction of the RhB molecules with the vanadium oxide layers in the xerogel.

4. Conclusions

The insoluble V_2O_5/TBO hybrid xerogel developed in this study showed a remarkable absorption capacity for RhB, reaching 179 $mg{\cdot}g^{-1}$. The sorption mechanism, predominantly driven by electrostatic forces between the positively charged RhB molecules and negatively charged hybrid xerogel surfaces, was proposed to explain this phenomenon. FTIR analysis proved the reduction of the $V_2O_5 \cdot nH_2O$ xerogel after being treated with TBO, as well as the intercalation of the RhB molecules within the lamellar structure of the hybrid xerogel. The increase in d-spacing in the hybrid xerogel from 11.58 Å to 19.24 Å after absorption of RhB (evaluated by XRD) further confirmed this phenomenon.

Acknowledgments

The authors gratefully acknowledge the research assistance of Wei Qiu and the University of Auckland Summer Research Scholarship for Mona Liu. The authors are also thankful to Higher Education Commission, Pakistan for scholarship grant for one of authors, Dr. Surayya Mukhtar for this research work.

Appendix A

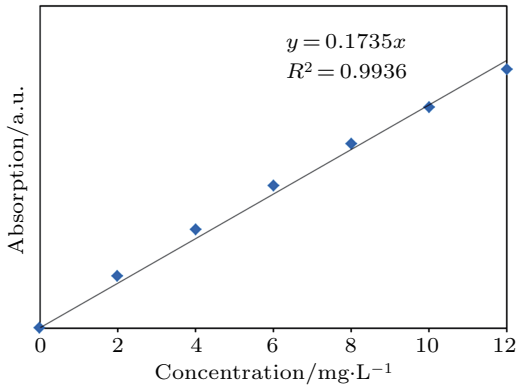


Fig. A1. (color online) Calibration curve for RhB aqueous solution measured by UV–Vis spectrophotometer.

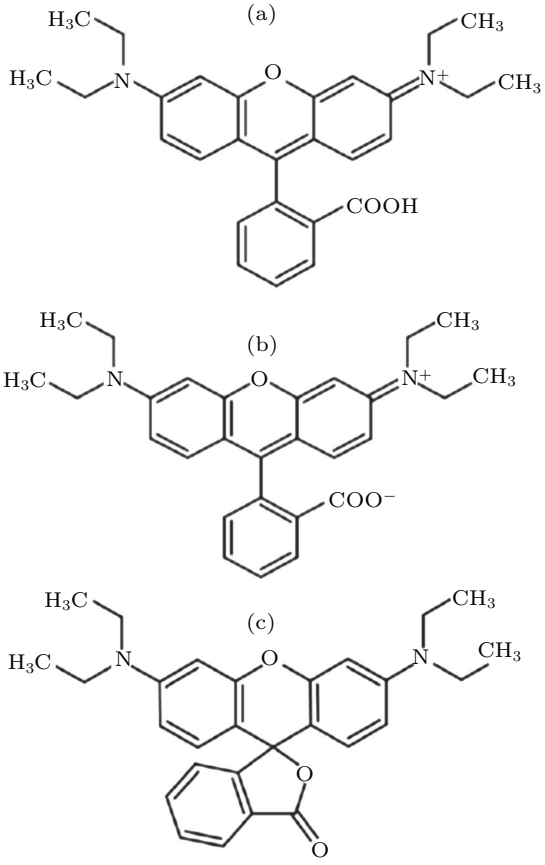


Fig. A2. Molecular structure and ionic forms of Rhodamine B: protonated RBH^+ (a) zwitterionic $RhB^{\pm}$ (b) and colorless lactone (c).[30,37]

References

[1] Churchman G J, Gates W P, Theng B K G and Yuan G 2006 Developments in Clay Science (Elsevier) p. 625
[2] Arbeloa F L, Martinez V M, Amer Chemical S O C and Arbeloa F L 2006 *Chem. Mater.* **18** 1407
[3] Lopez Arbeloa F 2007 *Journal of Photochemistry & Photobiology C: Photochemistry Reviews* **8** 85
[4] Bouraada M 2009 *J. Hazard. Mater.* **163** 463
[5] Bouraada M, Lafjah M, Ouali M S, de Menorval L C, Elsevier Science B V, Bouraada M, Lafjah M, Ouali M S, de Menorval L C and Ouali M S 2008 *J. Hazard. Mater.* **153** 911
[6] Almeida C A P, Debacher N A, Downs A J, Cottet L and Mello C A D 2009 *J. Colloid Interface Sci.* **332** 46

[7] Petkov V, Trikalitis P N, Bozin E S, Billinge S J L, Vogt T and Kanatzidis M G 2002 *JACS* **124** 10157
[8] Livage J 1991 *Chem. Mater.* **3** 578
[9] Jin A, Chen W, Zhu Q, Yang Y, Volkov V L and Zakharova G S 2008 *Solid State Ionics* **179** 1256
[10] Guerra E M, Ciuffi K J and Oliveira H P 2006 *J. Solid State Chem.* **179** 3814
[11] Liu Y J, DeGroot D C, Schindler J L, Kannewurf C R and Kanatzidis M G 1991 *Chemistry of Materials* **3** 992
[12] Shao L, Jeon J W and Lutkenhaus J L 2012 *Chem. Mater.* **24** 181
[13] Bouhaouss A and Aldebert P 1983 *Mater. Res. Bull.* **18** 1247
[14] Le D B, Passerini S, Coustier F, Guo J, Soderstrom T, Owens B B and Smyrl W H 1998 *Chem. Mater.* **10** 682
[15] Zakharova G S and Volkov V L 2003 *Russian Chemical Reviews* **72** 311
[16] Matsuo Y, Yamada N, Fukutsuka T, Sugie Y, Taylor, amp, Francis L T D, Matsuo Y and Fukutsuka T 2006 *Mol. Cryst. Liq. Cryst.* **452** 137
[17] Kuwahara T, Tagaya H and Kadokawa J-i 2001 *Inorg. Chem. Commun.* **4** 63
[18] Ackermans B, Schoonheydt R A and Ruiz-Hitzky E 1996 *Journal of the Chemical Society - Faraday Transactions* **92** 4479
[19] Kong A, Ding Y J, Wang P, Zhang H Q, Yang F and Shan Y K 2011 *J. Solid State Chem.* **184** 331
[20] Jang H Y, Quang-Thao T A, Ho X H and Sun-il M H O 2009 *Journal of the Korean Physical Society* **55** 2447
[21] Gharbi N, Sanchez C, Livage J, Lemerle J, Nejem L and Lefebvre J 1982 *Inorg. Chem.* **21** 2758
[22] Van Damme H, Letellier M, Tinet D, Kihal B and Erre R 1984 *Mater. Res. Bull.* **19** 1635
[23] Volkov V L, Zakharova G S, Kuznetsov M V, Jin A, Zhu Q and Chen W 2006 *Russian Journal of Inorganic Chemistry* **51** 1339
[24] Molochnikov L S, Zakharova G S, Mel'gunova E V and Volkov V L 2005 *Inorg. Mater.* **41** 1189
[25] Du G, Seng K H, Guo Z, Liu J, Li W, Jia D, Cook C, Liu Z and Liu H 2011 *RSC Advances* **1** 690
[26] Liu D, Liu Y, Pan A, Nagle K P, Seidler G T, Jeong Y-H and Cao G 2011 *The Journal of Physical Chemistry C* **115** 4959
[27] Lv S, Ding J, Peng H and Li G 2010 *Transition Met. Chem.* **35** 809
[28] Lee K and Cao G 2005 *J. Phys. Chem. B* **109** 11880
[29] Gad H M H and El-Sayed A A 2009 *J. Hazard. Mater.* **168** 1070
[30] Hamdi M H G 2009 *J. Hazard. Mater.* **168** 1070)
[31] Pospisil M, Capkova P, Weissmannova H, Klika Z, Trchova M, Chmielova M and Weiss Z 2003 *J. Mol. Model.* **9** 39
[32] Erre R, Masbah H, Crespin M, Van Damme H and Tinet D 1990 *Solid State Ionics* **37** 239
[33] Capkova P, Maly P, Pospıisil M, Klika Z, Weissmannova H and Weiss Z 2004 *J. Colloid Interface Sci.* **277** 128
[34] Klika Z, Weissmannova H, Capkova P and Pospisil M 2004 *J. Colloid Interface Sci.* **275** 243
[35] Subba Reddy C V, Jin A-P, Han X, Zhu Q-Y, Mai L-Q and Chen W 2006 *Electrochem. Commun.* **8** 279
[36] Imamura D, Miyayama M, Hibino M and Kudo T 2003 *J. Electrochem. Soc.* **150** A753
[37] Sagoo S K 2011 *Intrinsic Properties of Rhodamine B and Fluorescein Gas-phase Ions Studied Using Laser-induced Fluorescence and Photodissociation in a Quadrupole Ion Trap Mass Spectrometer* 2011: p. 25